Erratum

RINGO C is required to sustain the spindle-assembly checkpoint

Silvana Mourón, Guillermo de Cárcer, Esther Seco, Gonzalo Fernández-Miranda, Marcos Malumbres and Angel R. Nebreda

Journal of Cell Science 123, 2862

doi:10.1242/jcs.078493

There was an error in the first e-press version of the article published in *J. Cell Sci*. **123**, 2586-2595.

The corresponding author e-mail address was given incorrectly. The correct address is angel.nebreda@irbbarcelona.org.

The final online and print versions are correct. We apologise for this mistake.

RINGO C is required to sustain the spindle-assembly checkpoint

Silvana Mourón[1], Guillermo de Cárcer[2], Esther Seco[1], Gonzalo Fernández-Miranda[2], Marcos Malumbres[2] and Angel R. Nebreda[1,*,‡]

[1]Signalling and Cell Cycle Group and [2]Cell Division and Cancer Group, CNIO (Spanish National Cancer Center), Melchor Fernández Almagro 3, 28029 Madrid, Spain

*Present address: IRB-Barcelona, Baldiri Reixac 10, 08028 Barcelona, Spain
‡Author for correspondence (angel.nebreda@irbbarcelona.org)

Accepted 5 May 2010
Journal of Cell Science 123, 2586-2595

doi:10.1242/jcs.059964

Summary

RINGO/Speedy proteins are direct activators of Cdk1 and Cdk2 that have no sequence homology to cyclins. We have characterized the role in cell-cycle progression of a new human member of this protein family referred to as RINGO C. We show that siRNA-mediated knockdown of RINGO C results in premature mitotic exit with misaligned chromosomes, even in the presence of microtubule poisons. Time-lapse-microscopy experiments suggest that RINGO C is involved in the spindle-assembly checkpoint (SAC). Consistent with this idea, RINGO-C-depleted cells show impaired recruitment of the SAC components Mad2, Bub1 and BubR1. As the checkpoint is overridden, cells display defective chromosome segregation, which leads to an increased number of micronuclei and binucleated structures. Intriguingly, we found that RINGO C can associate with the mitotic kinase Aurora B, and downregulation of RINGO C produces mislocalization of the active form of Aurora B in prometaphase. Taken together, our results indicate a role for RINGO C in the mitotic checkpoint, which might be mediated by defective recruitment of SAC components and deregulation of the activity of Aurora kinase B.

Key words: Aurora kinase B, RINGO/Speedy mitosis, Spindle-assembly checkpoint

Introduction

Since mitosis was first described in the 1880s, scientists have tried to understand the molecular basis of chromosome segregation and the mechanisms that ensure genomic stability. Two major regulatory mechanisms of nuclear division are the activation of the Cdk1–cyclin-B-kinase complex that enforces mitosis entry, and the Cdc20-dependent activation of the anaphase-promoting complex/cyclosome (APC/C), a multi-subunit ubiquitin ligase that targets substrates for ubiquitylation and subsequent destruction by the proteasome triggering mitosis exit (Morgan, 1999; Nurse, 1990; Peters, 2006). However, the process needs several layers of control that switch on and off cell division at specific times and locations.

Aneuploidy is a hallmark of many types of cancers that can arise as a consequence of chromosome missegregation during cytokinesis. The spindle-assembly checkpoint (SAC) is a cell-cycle control mechanism that ensures the fidelity of chromosome segregation during mitosis by preventing premature entry into anaphase. This signal-transduction network is highly conserved from yeast to man, and includes the Mad, Bub and Mps1 proteins, which monitor different aspects of kinetochore-spindle interactions such as proper attachment between them or defects in the tension exerted by microtubule-generated forces on kinetochores (for reviews, see Kops et al., 2005; Musacchio and Salmon, 2007). Genetic mutation or changes in the expression levels of proteins such as BubR1 and Mad2 are associated with chromosomal instability (Cahill et al., 1998; Hanks et al., 2004; Kops et al., 2005; Shichiri et al., 2002).

The chromosomal passenger complex (CPC), so named for its dynamic localization pattern, includes the protein kinase Aurora B, INCENP, survivin and borealin. These proteins associate along the length of the condensing chromosomes in prophase, accumulate at the centromeres in prometaphase and metaphase, and relocate to the spindle midzone at anaphase onset before contracting in the midbody during cytokinesis. The complex has a pivotal role in chromosome congression, SAC function, chromosome segregation, central spindle formation and cytokinesis (for reviews, see Carmena and Earnshaw, 2003; Ruchaud et al., 2007). Aurora B is essential to resolve naturally occurring monopolar or syntelic microtubule-kinetochore attachments (Lampson et al., 2004; Tanaka et al., 2002), and to communicate a lack of bipolarity to the core SAC (Lens et al., 2003). Interference with the expression of any CPC component leads to a failure of CPC function in mitosis (Jeyaprakash et al., 2007; Lens et al., 2003; Ruchaud et al., 2007).

RINGO/Speedy proteins were initially identified as cell-cycle regulators that induce meiotic maturation in *Xenopus* oocytes. These proteins exhibit no amino acid sequence homology to cyclins, but can directly bind to and activate Cdk1 and Cdk2 (Ferby et al., 1999; Lenormand et al., 1999). Interestingly, RINGO-activated Cdk1 might contribute to meiosis I entry in oocytes by phosphorylating a particular set of residues in the Cdk1-cyclin B inhibitory kinase Myt1, which are poorly phosphorylated by CDK-cyclin complexes (Ruiz et al., 2008). The first human homologue, named Spy1 (herein referred to as RINGO A), is expressed in several human tissues and immortalized cell lines (Porter et al., 2002). Later, four additional mammalian homologues were identified and named RINGO B, RINGO C, RINGO D and RINGO E (Cheng et al., 2005; Dinarina et al., 2005; Nebreda, 2006). All RINGO/Speedy proteins contain a conserved central region, which is essential for CDK binding and activation (for reviews, see Gastwirt et al., 2007; Nebreda, 2006). However, very little is known of the function of mammalian RINGO/Speedy proteins,

with the exception of RINGO A, which has been proposed to have a role in G1-S progression via activation of Cdk2, as well as in the DNA-damage response, by inhibiting apoptosis and checkpoint activation (Barnes et al., 2003; Gastwirt et al., 2006). A recent study has also suggested the implication of RINGO C in the late-S and G2 phases of the cell cycle in HEK293 cells (Cheng and Solomon, 2008).

We show here that RINGO C is required to sustain the nocodazole- and taxol-induced mitotic arrest in human cells. In the absence of RINGO C, asynchronous cell cultures show impaired recruitment of SAC components and display chromosome misalignments and an increased number of micronuclei. The phenotypes induced upon downregulation of RINGO C resemble some of the effects observed when the CPC function is compromised. Interestingly, RINGO C associates with the mitotic kinase Aurora B in vitro and downregulation of RINGO C results in mislocalization of the active form of Aurora B.

Results

RINGO C is required for nocodazole-induced mitotic arrest

To investigate the function of RINGO C, we tested four siRNAs targeting different regions of the RINGO-C coding sequence. We found that oligos 2, 3 and 4 efficiently downregulated the endogenous RINGO C mRNA, as determined by quantitative RT-PCR, whereas oligo 1 only had a marginal effect (Fig. 1A, left). These results were confirmed by analyzing the ability of the different siRNAs to interfere with RINGO-C expression at the protein level (Fig. 1A, right). The interference with RINGO-C expression slightly reduced cell viability, as evaluated by the MTT assay (data not shown) but did not increase the proportion of apoptotic cells measured as the sub-G0 population in flow-cytometry analysis (supplementary material Fig. S1A).

As RINGO/Speedy proteins are known to bind to and activate Cdk1 and Cdk2, we used the siRNAs to investigate a possible role of RINGO C in cell-cycle regulation. When we analyzed by flow cytometry asynchronous cultures of RINGO-C-knockdown cells, we did not detect significant differences in the cell-cycle profile with respect to control cells (supplementary material Fig. S1A). RINGO C has been reported to bind to and activate both Cdk1 and Cdk2 (Dinarina et al., 2005), suggesting that it could be involved in mitosis. We therefore analyzed the role of RINGO C in a mitotic scenario using nocodazole, a spindle poison that interferes with microtubule polymerization and subsequently activates the SAC. We found that silencing of RINGO C largely prevented nocodazole-treated U2OS cells from arresting at prometaphase, as determined by staining with phospho-Ser10 histone H3 (H3-*P*) and MPM-2 antibodies in flow cytometry (Fig. 1B and supplementary material Fig. S1B), as well as in immunoblotting and immunofluorescence analysis (supplementary material Fig. S1C). In addition, we noticed an increased population of G1 cells upon treatment with siRNA to knock down RINGO C, especially when cells were incubated with nocodazole (Fig. 1B). These could represent cells that did not enter the cell cycle or that escaped from the nocodazole arrest. We focused our analysis on the mitotic phenotype and investigated the

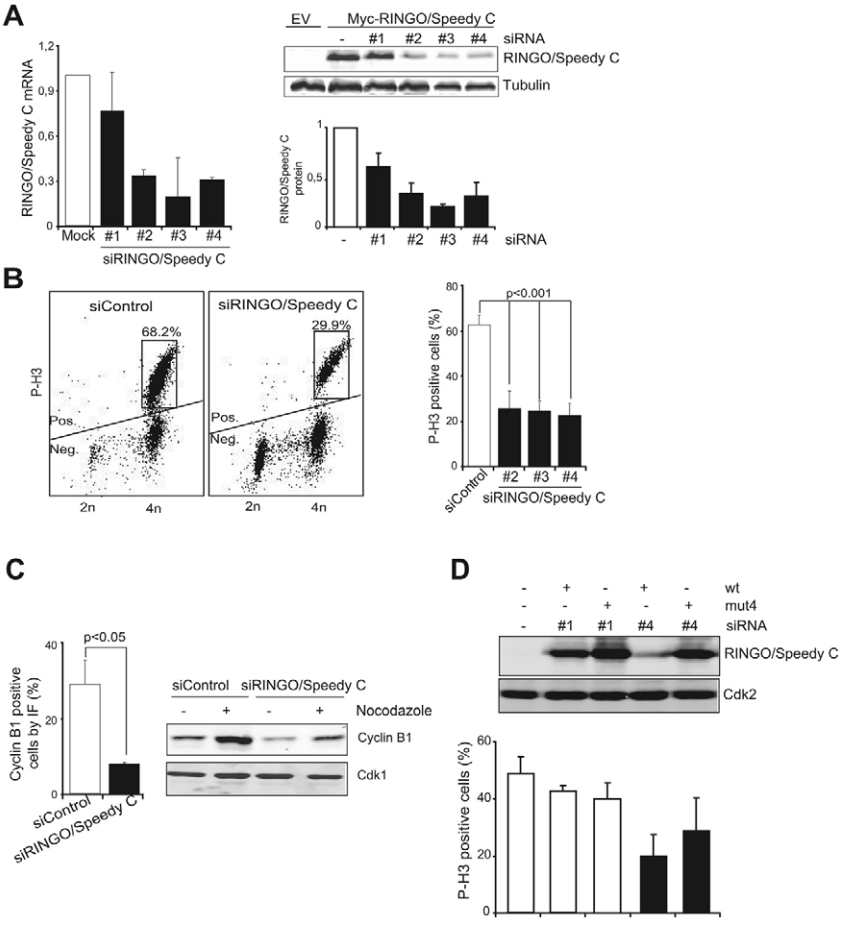

Fig. 1. RINGO C is required for nocodazole-induced metaphase arrest. (**A**) U2OS cells were transfected with siRNAs and 48 hours later, the endogenous levels of RINGO C mRNA were analyzed by qRT-PCR. The left histogram represents values normalized to *GAPDH*, expressed as mean ± s.d. of two different experiments performed in triplicate. The right panel shows an immunoblot of U2OS cells that were transfected first with 6×Myc-RINGO-C or the empty vector (EV) and 12 hours later with siRNAs. After 48 hours, cell lysates were analysed by immunoblotting. RINGO-C expression was normalized to the α-tubulin expression level in each sample and then referred to the expression level in mock-transfected cells. The histogram underneath represents the average RINGO-C protein levels normalized to α-tubulin from three experiments. (**B**) U2OS cells were transfected with siRNA to knock down RINGO C and incubated for 72 hours, of which the last 16 hours were in the presence of nocodazole. Mitotic cells were quantified by staining with propidium iodide and phosphorylated-Ser10 Histone 3 (P-H3) and analyzed by flow cytometry. The histogram represents mean ± s.d. of five independent experiments. (**C**) U2OS cells were transfected with the indicated siRNAs and incubated with nocodazole. The histogram represents average ± s.d. of the cyclin-B1-positive cells detected by indirect immunofluorescence in two experiments, counting about 500 cells in each (left panel). Total lysates of asynchronous and nocodazole-treated cells were also analyzed by immunoblotting (right panel). (**D**) U2OS cells were first transfected with constructs expressing either 6×Myc-RINGO-C WT or the mutant resistant to siRNA oligo 4 (mut 4) and 12 hours later with the indicated siRNAs. Two days later, the transfected cells were treated with nocodazole for 16 hours. The percentage of H3-*P*-positive cells was analyzed by FACs and represents the mean ± s.d. of two different experiments. Total cell lysates were also analyzed by immunoblotting.

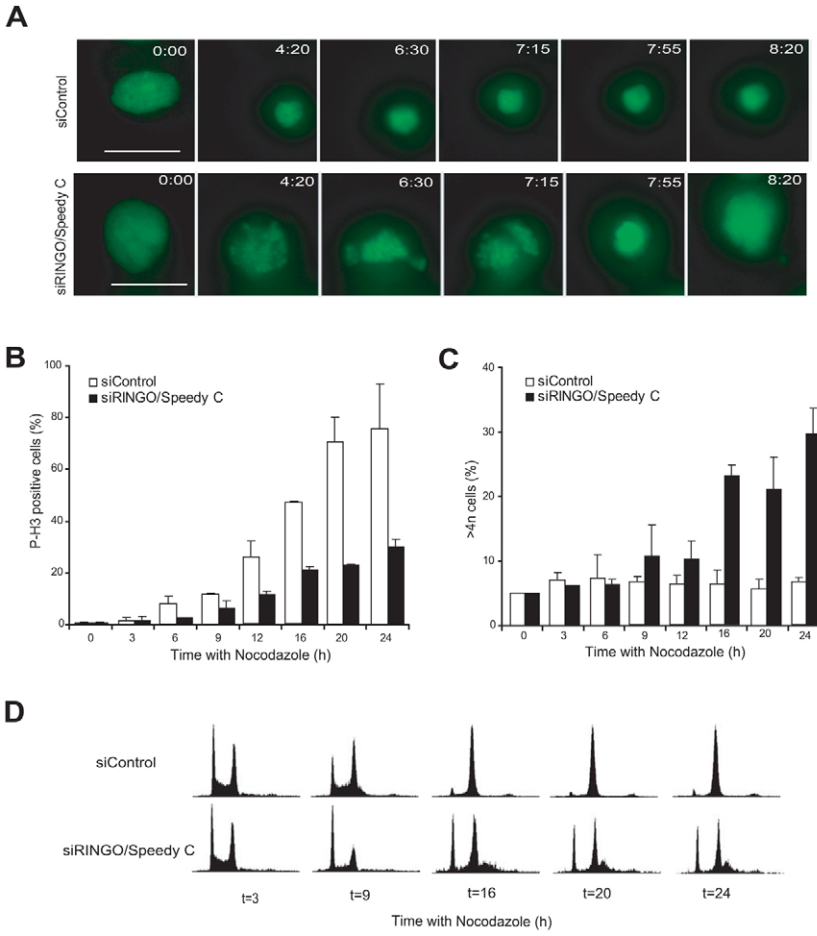

Fig. 2. Downregulation of RINGO C results in mitotic-checkpoint slippage. (**A**) Histone-4-GFP-expressing HeLa cells were transfected with control siRNA or siRNA to knock down RINGO C (oligo 4), synchronized with thymidine (2 mM) for 20 hours, released into fresh medium for 6 hours and then incubated in the presence of nocodazole for 16 hours. Cells were followed by time-lapse imaging every 5 minutes. Time indicated in the upper right corner indicates elapsed time (hours:minutes). Scale bar: 5 µm. (**B**) U2OS cells were transfected with the indicated siRNAs, treated with nocodazole for the indicated times and H3-*P*-positive cells were analyzed by FACs. The histogram represents mean ± s.d. of two different experiments. (**C**) The histogram indicates the proportion of cells with >4*n* DNA content from the flow cytometry analysis in B. (**D**) The DNA profiles show the increased polyploid cell population in RINGO-C-depleted cells quantified in C.

possibility that the observed overriding of the nocodazole-induced mitotic arrest was due to an impaired SAC function. This was supported by the treatment of RINGO-C-knockdown cells with taxol, a spindle toxin that activates the checkpoint by promoting microtubule stabilization. Again, RINGO-C downregulation interfered with the taxol-induced metaphase arrest of U2OS cells (supplementary material Fig. S1D). Similar results were obtained in HeLa cells treated with nocodazole (supplementary material Fig. S1E).

Another biochemical marker of mitosis is cyclin B1, which is present in cells from late G2 to metaphase but then is degraded before anaphase onset by the APC/C complex. The escape from mitosis of cells with compromised SAC results in the progressive destruction of cyclin B1. We confirmed that RINGO-C downregulation reduced the percentage of cyclin-B1-positive cells, as determined by both immunoblotting and immunofluorescence (Fig. 1C).

To validate the above results, we inserted two silent mutations in the RINGO C sequence that was targeted by the siRNA and verified that the mutant was resistant to downregulation (Fig. 1D). Importantly, expression of this RINGO-C mutant partially rescued the nocodozale-induced metaphase arrest in U2OS cells treated with the corresponding siRNA, as determined by quantification of H3-*P* staining, directly linking the impaired mitotic arrest with the specific downregulation of RINGO C. Taken together, these results suggest a mitotic function for RINGO C, which is probably associated with the SAC.

Downregulation of RINGO C produces a slippage of the mitotic checkpoint

To further characterize the implication of RINGO C in the SAC, we followed by time-lapse microscopy the mitotic progression of histone H4-GFP-expressing HeLa cells that were first synchronized with thymidine and then released into fresh medium in the presence of nocodazole. After the release from thymidine, cells re-enter the cell cycle and we know based on previous experiments, that about 6 hours later most of the cells start going through mitosis, which is when we started image acquisition. In contrast with the cells transfected with control siRNA, which were permanently arrested at prometaphase, we found that RINGO-C-knockdown cells were able to segregate chromosomes, even in the presence of nocodazole, and in some cases remained tetraploid cells owing to a failure in cytokinesis (Fig. 2A and supplementary material Movies 1 and 2). The mitotic slippage was also confirmed by FACS analysis of H3-*P*-positive cells, because the RINGO-C-knockdown cells entered mitosis, but were unable to accumulate and eventually exit mitosis (Fig. 2B). As a consequence, the percentage of aneuploid and polyploid cells with DNA content greater than 4*n* was increased in the RINGO-C-deficient cell population (Fig. 2C,D).

RINGO C does not regulate mitotic entry but is required for proper chromosome alignment

Besides a possible override of the SAC, another explanation for the inability of RINGO-C-deficient cells to accumulate in mitosis could be that they have problems entering mitosis, perhaps because

of a G1 arrest. To address this possibility, we synchronized HeLa cells expressing histone H4-GFP with thymidine and then followed by time-lapse imaging their mitotic progression after release. Cells were first imaged when chromosomes began to condense (prophase) and were monitored until the completion of cytokinesis. We observed that control cells started to enter mitosis 6 hours after release from the thymidine block and 42% of the cells (n=72) took between 30 and 60 minutes from nuclear envelope breakdown to complete anaphase; the remaining cells took longer than 60 minutes. RINGO-C-knockdown cells entered mitosis with similar kinetics, but tended to progress faster and the percentage of cells that took less than 60 minutes to complete mitosis rose to 54% (n=73) (Fig. 3A,B; see also supplementary material Movies 3 and 4). Whereas the majority of metaphase figures from control cells showed normal chromosome condensation and bipolar spindle structures, RINGO-C-knockdown cells displayed chromosome misalignments and/or defective spindle structures in 70% of the metaphases analyzed in asynchronous cultures (Fig. 3C). These defects often resulted in unequal chromosome segregation into multiple daughter cells. In other cases, the RINGO-C-knockdown cells attempted to divide but finally fused into a single cell.

To evaluate the specificity of the chromosome-misalignment phenotype observed after RINGO-C downregulation, we transfected U2OS cells first with GFP-tagged RINGO C, either WT or the mutant resistant to siRNA (mut 4), and then with control siRNA or siRNA to knock down RINGO C. We found that expression of the RINGO-C mutant, but not the WT protein, reduced the percentage of metaphases with misaligned chromosomes observed in RINGO-C-knockdown cells to almost control levels (supplementary material Fig. S2).

The mitotic abnormalities observed upon downregulation of RINGO C were often accompanied by the formation of micronuclei

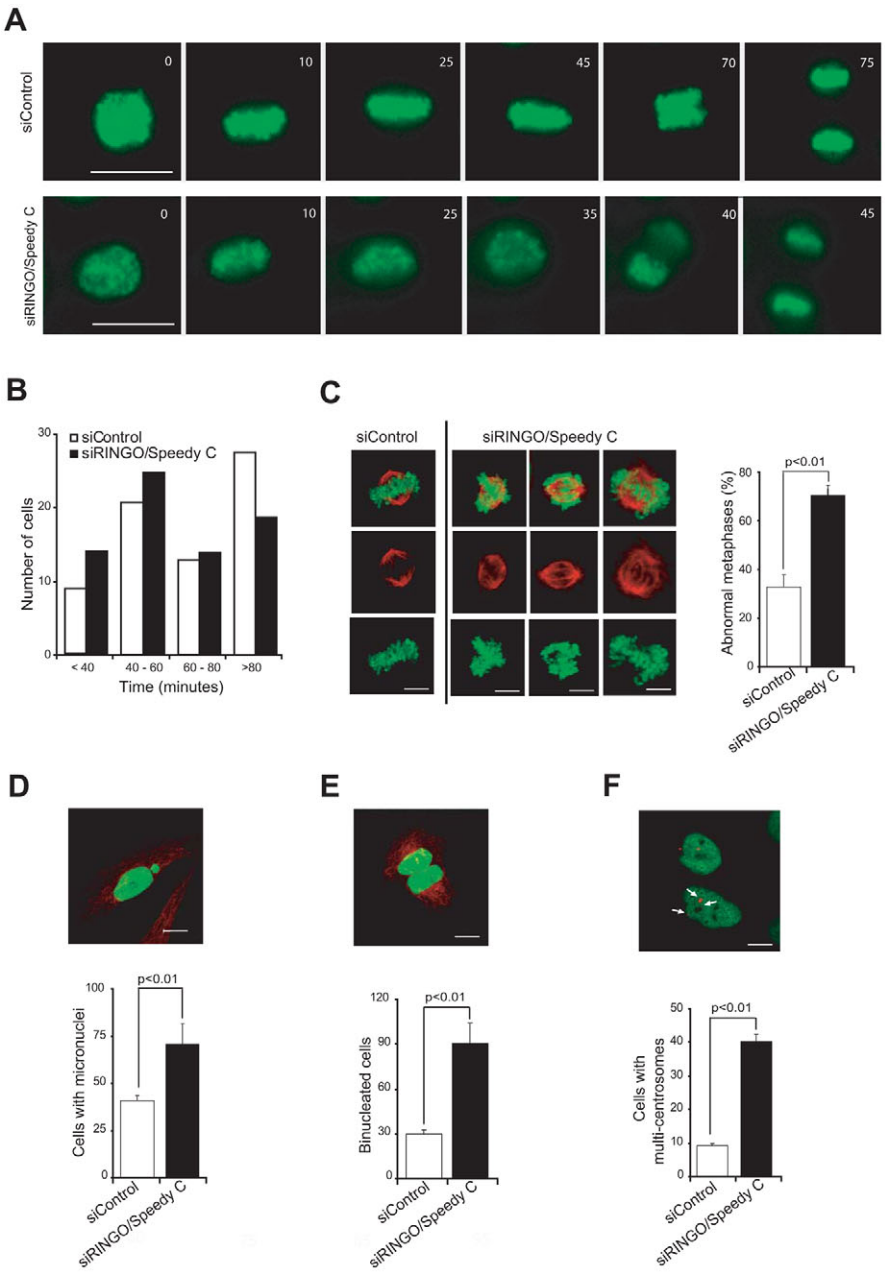

Fig. 3. RINGO C is not required for entry into mitosis. Histone-4-GFP-expressing HeLa cells were transfected with control siRNA or siRNA to knock down RINGO C (oligo 4) and 48 hours later were synchronized with thymidine for 20 hours, and then released into fresh medium. (**A**) Fluorescence time-lapse imaging was started 6 hours after release. Time in the upper right corner indicates the elapsed time (minutes) from the time of chromosome condensation to the completion of cytokinesis. Scale bar: 5 μm. (**B**) The histogram indicates the number of cells from the time-lapse analysis going from nuclear envelope breakdown to anaphase in different time periods. (**C**) Representative examples of cells showing misaligned chromosomes and abnormal microtubule spindles (red, α-tubulin; green, GFP). The histogram indicates the percentage of abnormal metaphases expressed as mean ± s.d. of three different experiments. Scale bars: 10 μm. (**D**,**E**) The number of cells with micronuclei and number of binucleated cells was determined by confocal microscopy. (**F**) Cells with supernumerary centrosomes were detected by immunofluorescence staining with γ-tubulin antibodies (red). Data in all panels represent mean ± s.d. of three different experiments (n=1000 cells in each experiment). Scale bars: 10 μm.

in G1 phase, which are usually derived from misaligned chromosomes (Fig. 3D), or by an increase in the number of binucleated cells owing to cytokinesis failure (Fig. 3E). Furthermore, the number of cells with numerous centrosomes, as detected by γ-tubulin staining, was about fourfold higher in RINGO-C-knockdown cells (Fig. 3F). Because supernumerary centrosomes were predominantly found in multinuclear cells, these findings point to cell division failures as the likely mechanism for the accumulation of centrosomes upon RINGO-C downregulation. Thus, although RINGO C is not required for mitosis entry, it seems to have an important role in allowing cells to properly align their chromosomes in the metaphase plate. Upon downregulation of RINGO C, cells exit mitosis prematurely, probably as a consequence of a defective SAC.

Impaired recruitment of SAC components to kinetochores upon downregulation of RINGO C

To investigate how RINGO C regulates chromosome alignment and checkpoint function, we analyzed the localization of the SAC components Mad2, BubR1 and Bub1 in prometaphases of asynchronous U2OS cells. These proteins typically localize as two discrete adjacent foci corresponding to the paired sister chromatid kinetochores, as expected when the SAC is active. However, the recruitment of SAC proteins to kinetochores was highly reduced in RINGO-C-knockdown cells (Fig. 4A,B). Another centromere-specific antibody, ACA, showed identical staining patterns in control and RINGO-C-knockdown cells, indicating that the absence of the SAC components from the centromeres was not due to loss of centromere structure. We also analysed kinetochore attachment, via depolymerization of microtubules using cold treatments and visualization of K-fibers by immunofluorescence, but found no evidence that the silencing of RINGO C affected proper kinetochore attachment to microtubules (supplementary material Fig. S3A). Importantly, co-transfection of a RINGO-C mutant resistant to siRNA rescued – to approximately control levels – the impaired recruitment of SAC proteins to centromeres observed upon downregulation of RINGO C (Fig. 4C). Recently, Mad2 has been found to be depleted by siRNAs directed against mRNA encoding

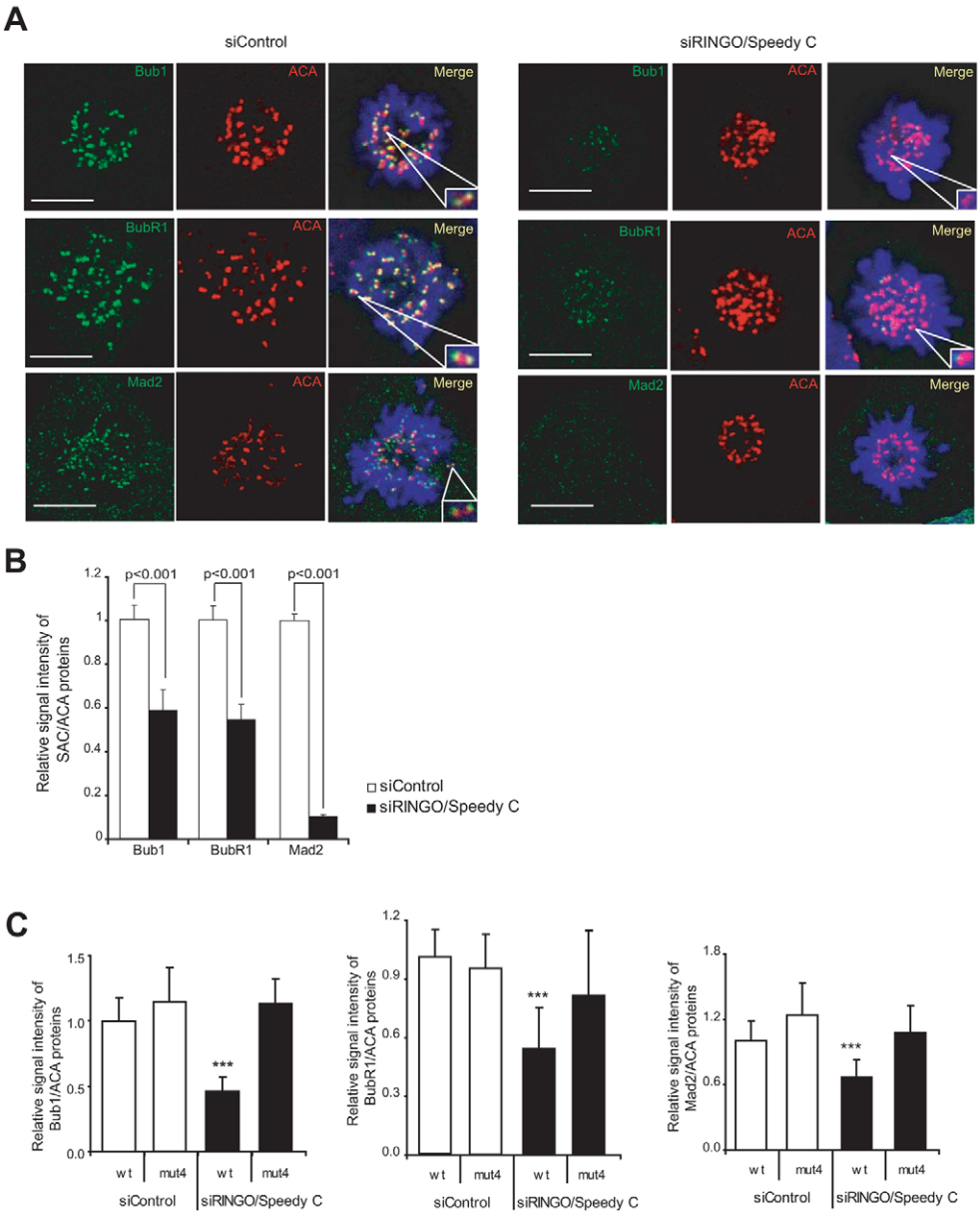

Fig. 4. Downregulation of RINGO C affects the localization of SAC components. (**A**) Immunolocalization of SAC components (green) and the centromeric protein ACA (red) in U2OS cells transfected with control siRNA or siRNA to knock down RINGO C (oligo 4). DNA was stained with DAPI (blue). Scale bars: 10 μm. (**B**) The histogram represents the relative signal intensity of SAC proteins/ACA (average ± s.d.) from 40 prometaphases of asynchronous cultures that were imaged using the same parameters of acquisition for cells transfected with control or RINGO C siRNAs. (**C**) The histogram represent the relative signal intensity of SAC proteins/ACA (average ± s.d.) from 30 prometaphases of asynchronous cultures that were imaged using the same parameters of acquisition for cells transfected with GFP-RINGO-C, either WT or mutant resistant to the siRNA oligo 4 (mut 4) and the indicated siRNAs (***P<0.001).

other proteins, leading to a misleading phenotype of SAC deficiency (Hübner et al., 2010; Westhorpe et al., 2010). To rule out this possibility, we performed immunoblotting and confirmed that total expression levels of the Mad2 protein were not affected in lysates of cells treated with siRNA designed to knock down RINGO C (supplementary material Fig. S3B).

These observations support the idea that RINGO-C downregulation affects the spindle checkpoint, because recruitment of checkpoint proteins to unattached kinetochores is necessary to maintain checkpoint signalling and to prevent precocious progression to anaphase.

Proteasome inhibition rescues SAC slippage induced by downregulation of RINGO C

A key event in the metaphase-anaphase transition is the Cdc20-dependent activation of the APC/C ubiquitin ligase, which triggers the degradation of the proteins cyclin B and securin, allowing exit from mitosis. Since SAC negatively regulates the activation of APC/C by Cdc20, the impairment of the SAC implies a premature activation of the APC/C complex, which in turn results in premature exit from mitosis.

To confirm that downregulation of RINGO C abrogates the SAC, we synchronized HeLa cells with nocodazole and then added the proteasome inhibitor MG132 for the last 3 hours. We found that the reduced levels of H3-*P*-positive cells observed upon RINGO-C downregulation were restored to about control levels when the cells were incubated with the proteasome inhibitor (Fig. 5A), suggesting that these cells were arrested in mitosis. We also found by confocal analysis of cultures released from a thymidine block, that incubation with MG132 increased the number of correctly aligned metaphase plates in RINGO-C-knockdown cells to the level seen in control cells (Fig. 5B). These results indicate that downregulation of RINGO C inhibits establishment of the SAC and consequently triggers premature APC/C activation.

RINGO C associates with Aurora kinase B

The mitotic defects observed upon RINGO-C downregulation were reminiscent of the phenotypes observed in cells depleted of Aurora B or other CPC components. To investigate the subcellular localization of the RINGO-C protein, U2OS cells were transfected with a GFP-tagged construct and were analyzed by confocal microscopy. We found that RINGO C was cytoplasmic during interphase and co-localized with γ-tubulin, suggesting some enrichment at the centrosomes. During mitosis, GFP-RINGO-C displayed an overall distribution with specific enrichment at the spindle poles and the midbody during telophase (Fig. 6A). Similar results were observed using Myc antibodies to detect Myc-tagged RINGO-C co-transfected with GFP-tagged Aurora kinase B (Fig. 6B).

Next, we investigated whether downregulation of RINGO C could affect the localization of endogenous Aurora B. We found that RINGO-C downregulation did not prevent the localization of total Aurora B to the centromeres and midbody (not shown). However, when we analyzed by immunofluorescence the localization of Aurora B phosphorylated on Thr232, an autophosphorylation site whose phosphorylation correlates with the activity of Aurora B, we observed that the active form of Aurora B was mislocalized in prometaphases and metaphases of RINGO-C-knockdown cells (Fig. 7A,B). By contrast, localization of Aurora B along the chromosome was not affected in RINGO-C-downregulated cells (supplementary material Fig. S4).

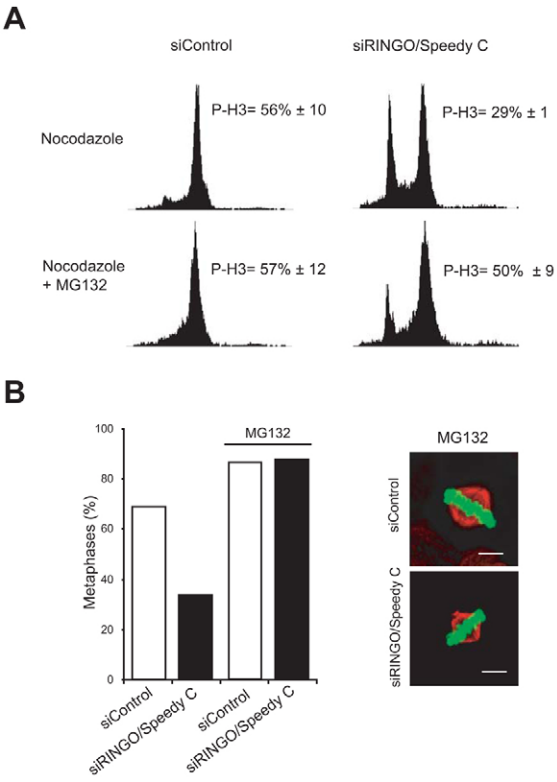

Fig. 5. Proteasome inhibition rescues RINGO-C-depleted cells from mitotic slippage. (**A**) HeLa cells were transfected with control siRNA or siRNA to knock down RINGO C (oligo 4) and then treated with nocodazole for 18 hours, of which the final 3 hours were in the presence of the proteasome inhibitor MG132 (25 μM) to inhibit the onset of anaphase. H3-*P*-positive cells were analyzed by FACS. Percentages represents the mean ± s.d. of two different experiments. (**B**) Histone 4-GFP-expressing HeLa cells were transfected with control siRNA or oligo 4 and 48 hours later were synchronized with thymidine for 20 hours, and then released into fresh medium for 8 hours. MG132 (25 μM) was added to the cells 3 hours before fixation. Cells stained with anti-α-tubulin antibodies (red) were analyzed by confocal microscopy. Scale bars: 10 μm. The histogram represents the percentage of normal metaphases in the mitotic figures observed by counting 1000 cells (left panel).

We then investigated the possible physical association between Aurora B and RINGO C. We found that Aurora B was present in the RINGO-C immunoprecipitates prepared from both asynchronous and nocodazole-treated cells (Fig. 8A). As the RINGO-C protein is known to associate with Cdk1 and Cdk2 (Cheng et al., 2005; Dinarina et al., 2005), we analyzed whether Aurora B associated with RINGO C directly or through its interaction with CDKs. For this purpose, we generated two RINGO C mutants in the conserved central core region, which should be impaired in CDK binding according to previous studies with other RINGO family members (Dinarina et al., 2005). We confirmed that indeed the RINGO-C mutants were unable to bind to Cdk1 and Cdk2 (Fig. 8B); however, GFP-Aurora-B was still co-immunoprecipitated with the two mutants (Fig. 8C). These results suggest that distinct RINGO-C domains are required for the interaction with Aurora B and CDKs.

To evaluate whether RINGO-C expression could affect activity of Aurora B in vivo, we analyzed the level of phosphorylation of

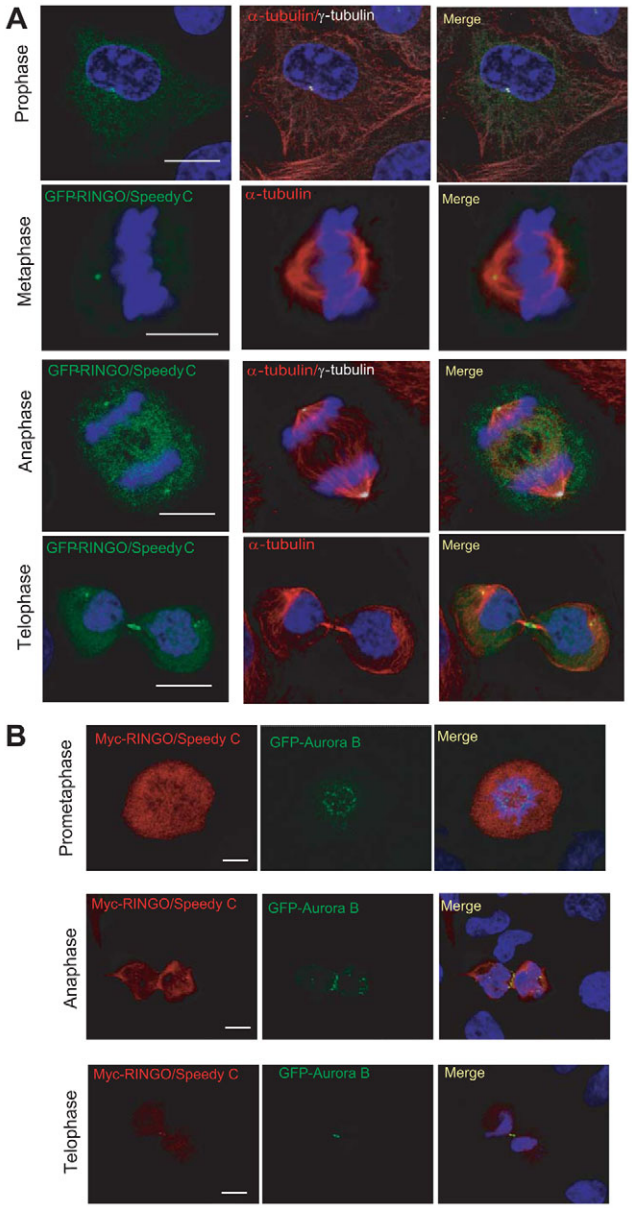

Fig. 6. RINGO C localizes to centrosomes and the midbody. (**A**) U2OS cells were transfected with GFP-RINGO-C and 2 days later were fixed, stained with anti-α-tubulin antibody (red) and DAPI (blue) and analyzed by confocal microscopy. Some of the samples were also stained with γ-tubulin antibody to confirm the colocalization with centrosome. (**B**) U2OS cells were co-transfected with 6×Myc-RINGO-C and GFP-Aurora-B and analyzed by confocal microscopy using anti-Myc antibody (red). Scale bars: 10 μm.

Aurora-B substrates by immunofluorescence. However, we observed no differences in intensities of staining for CENPA-*P* or H3-*P* between control and RINGO-C-downregulated cells (supplementary material Fig. S5). We also performed in vitro kinase assays using purified proteins but found no changes in activity of Aurora B upon incubation with RINGO C, either alone or with CDK1 (data not shown). These data suggest that knockdown of RINGO C leads to local defects in the function of Aurora B rather than to the direct inhibition of its kinase activity.

Discussion

We have shown that RINGO C has a role in the mitotic checkpoint response induced by drugs that interfere with microtubule polymerization and tension. Asynchronous cells treated with siRNAs to knock down RINGO C entered mitosis with normal kinetics, but exited mitosis faster than control cells and usually have misaligned chromosomes. This precocious exit is probably due to defective SAC function, because the recruitment of SAC components such as Bub1, BubR1 and Mad2 was impaired upon downregulation of RINGO C.

The SAC has an important role in the regulation of sister-chromatid separation and the proper attachment of chromosomes to spindle microtubules to prevent chromosomal instability due to unequal segregation of chromosomes during cell division. As cells enter mitosis, kinetochores constitutively generate signals that delay the activation of the APC/C and the onset of anaphase. These signals are gradually extinguished as sister kinetochores capture microtubules from opposite spindle poles and tension develops homogenously. Genetic mutations or changes in the expression levels of proteins involved in checkpoint signalling, such as BubR1 and Mad2, are associated with chromosomal instability and in some cases, predispose animals to spontaneous tumours (for a review, see Kops et al., 2005).

We confirmed that RINGO-C-knockdown cells have a defective SAC not only in normal mitosis but also when we used different spindle poisons. These experiments showed that RINGO C is crucial to sustain checkpoint arrest induced by drugs that affect tension (taxol) or disrupt microtubule-kinetochore attachments (nocodazole). SAC slippage is characterized by the precocious APC/C-mediated degradation of cyclin B and securin, two proteins that are necessary to inhibit the transition to anaphase. We have found that depletion of RINGO C results in significantly lower levels of cyclin B. Interestingly, when the anaphase onset was blocked by inhibiting proteasomal activity with MG132, we could rescue the expected levels of H3-*P* in RINGO-C-knockdown cells treated with nocodazole, and the levels of normal mitosis were also similar in controls and RINGO-C-knockdown cells. As a consequence of the impaired mitotic checkpoint, we showed that RINGO-C-knockdown cells displayed misalignment of chromosomes on the metaphase plate. The increased number of cells with micronuclei or binucleated was probably a consequence of the presence of lagging chromosomes and cytokinesis failure.

Our results partially resemble observations made upon downregulation of Aurora B and other components of the CPC. The expression of several CPC components has been shown to be essential for chromosome alignment and to sustain a checkpoint arrest induced by drugs that affect tension, such as taxol. The impaired SAC correlates with loss of both Mad2 and BubR1 from kinetochores in prometaphases of cells lacking survivin (Lens et al., 2003). Aurora B activity is not only required for SAC function, but also for correct chromosome alignment (Ditchfield et al., 2003; Hauf et al., 2003; Vader et al., 2007). Chemical inhibition of Aurora B activity with ZM447439 produced abnormal chromosome alignment, and severely affected the kinetochore localization of both BubR1 and Mad2 (Ditchfield et al., 2003). RNAi-mediated downregulation of Aurora B also reduced the accumulation of mitotic cells after spindle damage, and inhibited the kinetochore localization of BubR1, Mad2 and Cenp-E (Ditchfield et al., 2003). Recently, Gö6976 has been described as a novel pharmacologic inhibitor of the SAC, which targets Aurora B activity. Interestingly, Gö6976 treatment induces rapid exit from mitosis in the presence

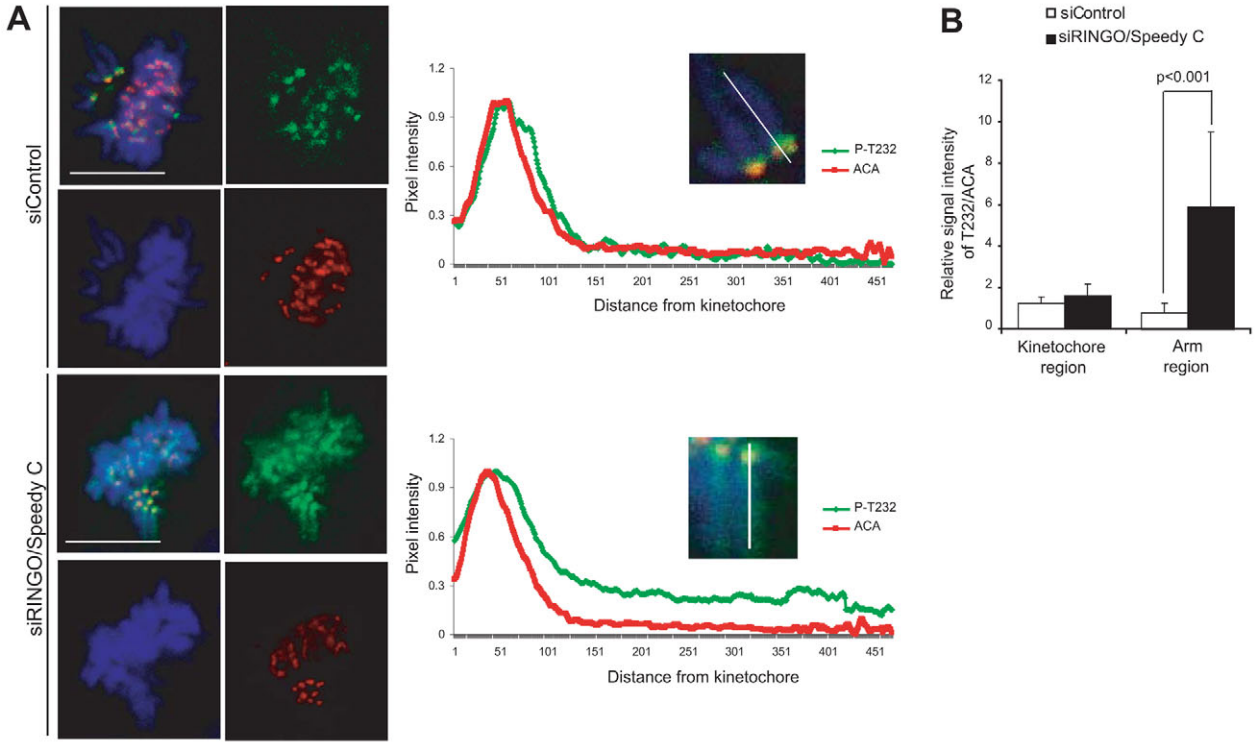

Fig. 7. Downregulation of RINGO C affects the localization of active Aurora B. (**A**) U2OS cells were transfected with control siRNA or siRNA to knock down RINGO C (oligo 4) and the localization of the active form of Aurora B phosphorylated on T232 was analyzed by immunofluorescence. The centromeric localization was determined by co-staining with anti-ACA antibodies (left panels). To quantify the mislocalization, a line was drawn along the chromosome and the intensity of both phosphorylated T232 Aurora B (green) and ACA (red) was measured. The graphs represent the quantification of staining for both phosphorylated T232 Aurora B (green) and ACA (red) in 20 chromosomes from 20 different cells. Scale bars: 10 µm. (**B**) Relative signal intensity of phospho-T232 Aurora B and ACA both in the kinetochore (considered as the first quartile of the total pixel intensities along the chromosome) and in the arm region (rest of the chromosome).

of either nocodazole or taxol, which correlates with impaired kinetochore localization of Bub1 and BubR1, as well as with mislocalization of Aurora B from the centromere region to chromosome arms (Stolz et al., 2009).

Taken together, our data suggest a role for RINGO C in the control of the SAC, at least in part through the regulation of the function of Aurora B. The activation of Aurora B at the centromeres is regulated at many levels (Jelluma et al., 2008; Kelly et al., 2007;

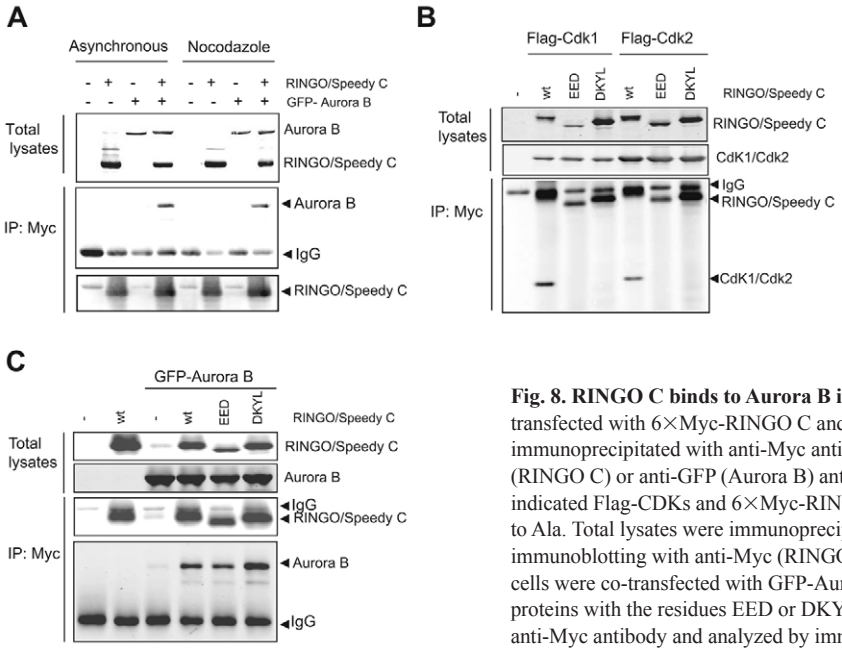

Fig. 8. RINGO C binds to Aurora B independently of CDKs. (**A**) HEK293T cells were co-transfected with 6×Myc-RINGO C and GFP-Aurora-B and 2 days later cell lysates were immunoprecipitated with anti-Myc antibody and analyzed by immunoblotting with anti-Myc (RINGO C) or anti-GFP (Aurora B) antibodies. (**B**) HEK293T cells were co-transfected with the indicated Flag-CDKs and 6×Myc-RINGO C, either WT or with the residues EED or DKYL mutated to Ala. Total lysates were immunoprecipitated with anti-Myc antibody and analyzed by immunoblotting with anti-Myc (RINGO C) or anti-GFP (Cdk1 and Cdk2) antibodies. (**C**) HEK293T cells were co-transfected with GFP-Aurora B and the indicated 6×Myc-RINGO-C WT and mutant proteins with the residues EED or DKYL mutated to Ala. Total lysates were immunoprecipitated with anti-Myc antibody and analyzed by immunoblotting as in A.

Sessa et al., 2005). We show that RINGO C is not required for loading of Aurora B onto centromeres, but it is somehow required for the proper localization of the Thr232-phosphorylated form of Aurora B. However, we could find no evidence that the overall Aurora B activity is affected, at least regarding the phosphorylation of CENPA and H3 substrates. One possibility is that RINGO C modulates the poorly characterized pathways that control the timely removal of Aurora B from the chromosome arms (Sumara et al., 2007) or perhaps regulate the disengagement of Aurora B from other CPC partners at this stage. Any defect in the dynamics of localization of Aurora B at chromosomes is likely to have consequences in the SAC. Based on previous findings indicating that the activation of Cdk1 and Cdk2 has a major role in the functions of RINGO proteins (for reviews, see Gastwirt et al., 2007; Nebreda, 2006), it is possible also that the mitotic role of RINGO C is mediated by CDK activation. In fact, Cdk1 impinges both on Aurora B activity and CPC function (Goto et al., 2006), as well as on the proper function of SAC effectors such as Bub1, BubR1 and Mad2 (Qi et al., 2006; Wong and Fang, 2007). The observation that RINGO C can bind to Aurora B in a CDK-independent manner, does not exclude the possibility that RINGO C-activated CDKs could regulate Aurora B. For example, the Cdk1/XRINGO substrate Myt1 can bind to XRINGO independently of CDKs (Ruiz et al., 2008). Thus, RINGO C could link Cdk1 and Aurora B activity for proper SAC function; an attractive hypothesis that will require further investigation.

Materials and Methods

DNA constructs

RINGO C was cloned in the pCS+MT vector using *Xho*I to express a protein N-terminally tagged with 6×Myc. GFP-fused RINGO C was generated by cloning the cDNA in pEGFP-C2 using *Bam*HI. To obtain a RINGO C mutant resistant to the RNAi oligo 4, we introduced two silent mutations in the corresponding target sequence by PCR-based mutagenesis using the QuikChange® site-directed mutagenesis kit (Stratagene), as follows: CTGTACCTCGCAAATGACA (oligo 4). The 6×Myc-tagged RINGO C mutants impaired in CDK binding were generated by PCR-based mutagenesis as described (Dinarina et al., 2005). Flag-tagged CDKs were cloned in the pCDNA3 vector using *Bam*HI and *Xho*I.

cDNA encoding Aurora B was amplified by PCR from the plasmid mAA0155 (Mammalian Gene Collection), cloned into pENTR-D-TOPO vector using TOPO technology (Invitrogen) and transferred to a destiny vector coexpressing GFP by a LR recombination reaction of the Gateway system (Invitrogen).

Short interfering RNA (siRNA)

The following siRNA oligos (Dharmacon) were used to target RINGO C: oligo 1, 5′-TGAAGCTCAGCGAGTATAC-3′, oligo 2, 5′-TTAAGCCTGTGTCATCCAA-3′, oligo 3, 5′-TCCAGATTTCAGATAAGTA-3′ and oligo 4, 5′-CTGTAC-CTTGCAAACGACA-3′.

Cell culture and transfection

HEK293T, U2OS and HeLa cells were maintained in DMEM medium supplemented with 10% fetal bovine serum and antibiotics and were grown at 37°C in a humidified 5% CO_2 atmosphere. For immunoblotting, cells were seeded at 50-60% confluence in 10 cm plates and were transfected with 6 μg plasmid DNA using FuGENE®6 transfection reagent (Roche) according to the manufacturer's instructions. For immunoprecipitations, HEK293T cells were transfected with 6 μg plasmid DNA by the standard calcium phosphate transfection protocol. For silencing experiments, cells were transfected with 100 nM oligos using DharmaFECT™ 1 siRNA transfection reagent (Dharmacon) according to the manufacturer's instructions. For immunofluorescence experiments, cells were seeded onto coverslips and transfected at 50-60% confluence with 1 μg plasmid DNA using FuGENE®6 transfection reagent or 100 nM siRNA oligos using DharmaFECT™ 1 siRNA transfection reagent. For time-lapse experiments, HeLa cells stably expressing Histone 4-GFP were seeded after 48 hours of transfection with siRNA oligos on a four-chamber plate (Lab-TekII).

Real-time RT-PCR

U2OS cells were transfected with siRNA oligos and 48 hours later, total RNA was extracted with Trizol (Invitrogen), treated with DNase and purified using a phenol-chloroform protocol. cDNA synthesis was performed using random primers with 4 μg total RNA and SuperScript II (Invitrogen). PCR was performed with Power SYBR Green PCR Master Mix (Applied Biosystems).

Antibodies

The following primary antibodies were used: human anti-ACA (Antibodies Incorporated), mouse anti-Aurora B (BD Biosciences), rabbit anti-phospho-Thr232 Aurora B (Rockland), mouse anti-Bub1 (MBL), mouse anti-BubR1 (MBL), mouse anti-Cdk1 (Santa Cruz), rabbit anti-Cdk2 (Santa Cruz), rabbit anti-cyclin B1 (Santa Cruz), mouse anti-FLAG (Upstate), mouse anti-GFP (Sigma), mouse anti-Mad2 (MBL), mouse anti-MPM2 (Upstate), mouse anti-c-Myc (Santa Cruz), rabbit anti-phospho-Ser7 CENP-A (Upstate), rabbit anti-phospho-Ser10 Histone 3 (Upstate), mouse anti-α-tubulin (Roche), γ-tubulin (Sigma). The secondary antibodies were purchased from Invitrogen Molecular Probes (goat anti-rabbit IgG Alexa Fluor 555, chicken anti-rabbit IgG Alexa Fluor 594, chicken anti-rabbit IgG Alexa Fluor 488, goat anti-mouse IgG Alexa Fluor 555, goat anti-mouse IgG Alexa Fluor 594, goat anti-mouse IgG Alexa Fluor 488, donkey anti-mouse IgG Alexa Fluor 647, goat anti-mouse IgG Alexa Fluor 680, goat anti-rabbit IgG Alexa Fluor 680) or from Rockland (donkey anti-mouse IgG Li-Cor IRDye 800 and goat anti-rabbit IgG Li-Cor IRDye 800).

Cell synchronization and flow cytometry

For cell synchronization at the G1-S transition, cells were incubated with thymidine (2 mM, Sigma) for 20 hours. To arrest cells in prometaphase, asynchronous cells were treated with 100 nM nocodazole (Sigma) or 1 μM Paclitaxel (Sigma T-7402) for 16 hours. In some experiments, nocodazole was added 6 hours after release of cells from the thymidine block. To inhibit protein degradation, cells were treated with the proteasomal inhibitor MG132 (25 μM, Sigma) for 3 hours. The percentage of mitotic cells (H3-*P* positive) and the cell-cycle distribution (DNA stained with propidium iodide, Sigma) were determined by flow cytometry on a FACScalibur flow cytometer (Becton Dickinson), and data were processed using CellQuest software.

Immunofluorescence confocal microscopy

Cells were grown on coverslips, washed twice with PBS and fixed for 10 minutes in PTEMP buffer (20 mM PIPES pH 6.8, 0.2% Triton X-100, 10 mM EGTA and 1 mM $MgCl_2$) containing 4% paraformaldehyde. After washing twice with PBS, coverslips were kept in methanol at –20°C. For immunofluorescence staining, coverslips were washed twice with PBS, and then blocked in PBS with 1% bovine serum albumin for 30 minutes before the indicated primary antibody was applied. Cells were then washed with PBS and incubated with Alexa Fluor 488-, 555-, 594- or 647-conjugated secondary antibody (Molecular Probes). Cell nuclei were stained with DAPI (Sigma). After washing, coverslips were mounted onto glass microscope slides with Mowiol (Calbiochem). Images were acquired using Leica-TCS SP2 AOBS confocal microscope, with a HCX PL APO 63× 1.4 NA oil-immersion objective using LCS version 2.61 software. For centromeric proteins and ACA ratio calculations, ACA staining was used to define kinetochore or centromere regions in the Z-plane and ACA intensity was used as constant reference for the kinetochore or centromere signal. For each condition, 40 cells were quantified using Metamorph software (Universal Imaging Corporation). For calculations of the ratio of phosphorylated T232 Aurora B to ACA, ACA staining was used to define kinetochore and centromere regions. The intensity of both Aurora B and ACA was obtained by drawing a line along the chromosome and measuring the intensity of staining using LCS version 2.61 software.

Time-lapse analysis

For time-lapse videomicroscopy, HeLa cells stably expressing Histone H4-GFP were plated on 35 mm plates and transfected with siRNA oligos. After 48 hours, cells were split on camera chambers and incubated with thymidine for 20 hours. Cells were followed by time-lapse microscopy starting 6 hours after release in fresh medium or in the presence of nocodazole for 16 hours. Image acquisition was performed using a Delta-vision fluorescence microscope (Applied Precision) equipped with a selective filter for GFP emission and a UPLanFLN 40× 1.3 NA oil-immersion objective. GFP images were acquired at 5 minute intervals using SoftWoRx version 3.4.2 software.

Cold-stable K-fibers

For K-fiber visualization, U2OS cells were incubated for 10 minutes in ice-cold L-15 medium (Invitrogen) with 20 mM HEPES, pH 7.3, as previously described (Gassmann et al., 2007). Cells were then fixed for 10 minutes at room temperature with 4% formaldehyde in 100 mM PIPES, pH 6.8, 10 mM EGTA, 1 mM $MgCl_2$ and 0.2% Triton X-100. Cells were then processed for indirect immunofluorescence.

Immunoprecipitation and immunoblotting

For immunoblotting, cellular proteins were solubilized in lysis buffer (50 mM Tris-HCl, pH 7.5, 150 mM NaCl, 1% NP-40, 5 mM EDTA, 5 mM EGTA, 20 mM NaF, 0.1 μM PMSF, 0.5 μM benzamidine, 1 μg/μl leupeptin, 1 μg/μl aprotinin, 2 μM microcystin and 0.1 μM $NaVO_3$), boiled for 5 minutes and analyzed by SDS-PAGE using Laemmli gels. The blots were developed using Alexa Fluor 680- or Li-Cor IRDye 800-labelled antibodies with the Odyssey Infrared Imaging System (Li-Cor).

For RINGO C immunoprecipitation, total lysates were incubated with anti-Myc antibody for 2 hours at 4°C on a rotating wheel. Immune complexes were collected with Protein-G-agarose beads (Santa Cruz), washed twice with lysis buffer and processed for immunoblotting.

We thank Diego Megias (Confocal Microscopy Unit, CNIO) for his help in the acquisition and quantification of confocal microscope images and time-lapse analysis. This work was funded by CNIO and by grants BFU2004-03566, RD06/0020/0083, CSD2007-00017, SAF2006-05186 and SAF2009-07973 from the Spanish Ministerio de Ciencia e Innovación (MICINN), and S-BIO-0283-2006 from the Comunidad de Madrid. S.M. was supported by CNIO and by a Juan de la Cierva postdoctoral contract from MICINN.

Supplementary material available online at
http://jcs.biologists.org/cgi/content/full/123/15/2586/DC1

References

Barnes, E. A., Porter, L. A., Lenormand, J. L., Dellinger, R. W. and Donoghue, D. J. (2003). Human Spy1 promotes survival of mammalian cells following DNA damage. *Cancer Res.* **63**, 3701-3707.

Cahill, D. P., Lengauer, C., Yu, J., Riggins, G. J., Willson, J. K., Markowitz, S. D., Kinzler, K. W. and Vogelstein, B. (1998). Mutations of mitotic checkpoint genes in human cancers. *Nature* **392**, 300-303.

Carmena, M. and Earnshaw, W. C. (2003). The cellular geography of aurora kinases. *Nat. Rev. Mol. Cell Biol.* **4**, 842-854.

Cheng, A. and Solomon, M. J. (2008). Speedy/Ringo C regulates S and G2 phase progression in human cells. *Cell Cycle* **7**, 3037-3047.

Cheng, A., Xiong, W., Ferrell, J. E., Jr and Solomon, M. J. (2005). Identification and comparative analysis of multiple mammalian Speedy/Ringo proteins. *Cell Cycle* **4**, 155-165.

Dinarina, A., Perez, L. H., Davila, A., Schwab, M., Hunt, T. and Nebreda, A. R. (2005). Characterization of a new family of cyclin-dependent kinase activators. *Biochem. J.* **386**, 349-355.

Ditchfield, C., Johnson, V. L., Tighe, A., Ellston, R., Haworth, C., Johnson, T., Mortlock, A., Keen, N. and Taylor, S. S. (2003). Aurora B couples chromosome alignment with anaphase by targeting BubR1, Mad2, and Cenp-E to kinetochores. *J. Cell Biol.* **161**, 267-280.

Ferby, I., Blazquez, M., Palmer, A., Eritja, R. and Nebreda, A. R. (1999). A novel p34(cdc2)-binding and activating protein that is necessary and sufficient to trigger G(2)/M progression in Xenopus oocytes. *Genes Dev.* **13**, 2177-2189.

Gassmann, R., Kline, S. L., Carvalho, A. and Desai, A. (2007). Analysis of kinetochore assembly and function in Caenorhabditis elegans embryos and human cells. *Methods* **41**, 177-189.

Gastwirt, R. F., Slavin, D. A., McAndrew, C. W. and Donoghue, D. J. (2006). Spy1 expression prevents normal cellular responses to DNA damage: inhibition of apoptosis and checkpoint activation. *J. Biol. Chem.* **281**, 35425-35435.

Gastwirt, R. F., McAndrew, C. W. and Donoghue, D. J. (2007). Speedy/RINGO regulation of CDKs in cell cycle, checkpoint activation and apoptosis. *Cell Cycle* **6**, 1188-1193.

Goto, H., Kiyono, T., Tomono, Y., Kawajiri, A., Urano, T., Furukawa, K., Nigg, E. A. and Inagaki, M. (2006). Complex formation of Plk1 and INCENP required for metaphase-anaphase transition. *Nat. Cell. Biol.* **8**, 180-187.

Hanks, S., Coleman, K., Reid, S., Plaja, A., Firth, H., Fitzpatrick, D., Kidd, A., Mehes, K., Nash, R., Robin, N. et al. (2004). Constitutional aneuploidy and cancer predisposition caused by biallelic mutations in BUB1B. *Nat. Genet.* **36**, 1159-1161.

Hauf, S., Cole, R. W., LaTerra, S., Zimmer, C., Schnapp, G., Walter, R., Heckel, A., van Meel, J., Rieder, C. L. and Peters, J. M. (2003). The small molecule Hesperadin reveals a role for Aurora B in correcting kinetochore-microtubule attachment and in maintaining the spindle assembly checkpoint. *J. Cell Biol.* **161**, 281-294.

Hübner, N. C., Wang, L. H., Kaulich, M., Descombes, P., Poser, I. and Nigg, E. A. (2010). Re-examination of siRNA specificity questions role of PICH and Tao1 in the spindle checkpoint and identifies Mad2 as a sensitive target for small RNAs. *Chromosoma* **119**, 149-165.

Jelluma, N., Brenkman, A. B., van den Broek, N. J., Cruijsen, C. W., van Osch, M. H., Lens, S. M., Medema, R. H. and Kops, G. J. (2008). Mps1 phosphorylates Borealin to control Aurora B activity and chromosome alignment. *Cell* **132**, 233-246.

Jeyaprakash, A. A., Klein, U. R., Lindner, D., Ebert, J., Nigg, E. A. and Conti, E. (2007). Structure of a Survivin-Borealin-INCENP core complex reveals how chromosomal passengers travel together. *Cell* **131**, 271-285.

Kelly, A. E., Sampath, S. C., Maniar, T. A., Woo, E. M., Chait, B. T. and Funabiki, H. (2007). Chromosomal enrichment and activation of the aurora B pathway are coupled to spatially regulate spindle assembly. *Dev. Cell* **12**, 31-43.

Kops, G. J., Weaver, B. A. and Cleveland, D. W. (2005). On the road to cancer: aneuploidy and the mitotic checkpoint. *Nat. Rev. Cancer* **5**, 773-785.

Lampson, M. A., Renduchitala, K., Khodjakov, A. and Kapoor, T. M. (2004). Correcting improper chromosome-spindle attachments during cell division. *Nat. Cell Biol.* **6**, 232-237.

Lenormand, J. L., Dellinger, R. W., Knudsen, K. E., Subramani, S. and Donoghue, D. J. (1999). Speedy: a novel cell cycle regulator of the G2/M transition. *EMBO J.* **18**, 1869-1877.

Lens, S. M., Wolthuis, R. M., Klompmaker, R., Kauw, J., Agami, R., Brummelkamp, T., Kops, G. and Medema, R. H. (2003). Survivin is required for a sustained spindle checkpoint arrest in response to lack of tension. *EMBO J.* **22**, 2934-2947.

Morgan, D. O. (1999). Regulation of the APC and the exit from mitosis. *Nat. Cell Biol.* **1**, E47-E53.

Musacchio, A. and Salmon, E. D. (2007). The spindle-assembly checkpoint in space and time. *Nat. Rev. Mol. Cell Biol.* **8**, 379-393.

Nebreda, A. R. (2006). CDK activation by non-cyclin proteins. *Curr. Opin. Cell Biol.* **18**, 192-198.

Nurse, P. (1990). Universal control mechanism regulating onset of M-phase. *Nature* **344**, 503-508.

Peters, J. M. (2006). The anaphase promoting complex/cyclosome: a machine designed to destroy. *Nat. Rev. Mol. Cell Biol.* **7**, 644-656.

Porter, L. A., Dellinger, R. W., Tynan, J. A., Barnes, E. A., Kong, M., Lenormand, J. L. and Donoghue, D. J. (2002). Human Speedy: a novel cell cycle regulator that enhances proliferation through activation of Cdk2. *J. Cell Biol.* **157**, 357-366.

Qi, W., Tang, Z. and Yu, H. (2006). Phosphorylation- and polo-box-dependent binding of Plk1 to Bub1 is required for the kinetochore localization of Plk1. *Mol. Biol. Cell* **17**, 3705-3716.

Ruchaud, S., Carmena, M. and Earnshaw, W. C. (2007). Chromosomal passengers: conducting cell division. *Nat. Rev. Mol. Cell Biol.* **8**, 798-812.

Ruiz, E. J., Hunt, T. and Nebreda, A. R. (2008). Meiotic inactivation of Xenopus Myt1 by CDK/XRINGO, but not CDK/cyclin, via site-specific phosphorylation. *Mol. Cell* **32**, 210-220.

Sessa, F., Mapelli, M., Ciferri, C., Tarricone, C., Areces, L. B., Schneider, T. R., Stukenberg, P. T. and Musacchio, A. (2005). Mechanism of Aurora B activation by INCENP and inhibition by hesperadin. *Mol. Cell* **18**, 379-391.

Shichiri, M., Yoshinaga, K., Hisatomi, H., Sugihara, K. and Hirata, Y. (2002). Genetic and epigenetic inactivation of mitotic checkpoint genes hBUB1 and hBUBR1 and their relationship to survival. *Cancer Res.* **62**, 13-17.

Stolz, A., Vogel, C., Schneider, V., Ertych, N., Kienitz, A., Yu, H. and Bastians, H. (2009). Pharmacologic abrogation of the mitotic spindle checkpoint by an indolocarbazole discovered by cellular screening efficiently kills cancer cells. *Cancer Res.* **69**, 3874-3883.

Sumara, I., Quadroni, M., Frei, C., Olma, M. H., Sumara, G., Ricci, R. and Peter, M. (2007). A Cul3-based E3 ligase removes Aurora B from mitotic chromosomes, regulating mitotic progression and completion of cytokinesis in human cells. *Dev. Cell* **12**, 887-900.

Tanaka, T. U., Rachidi, N., Janke, C., Pereira, G., Galova, M., Schiebel, E., Stark, M. J. and Nasmyth, K. (2002). Evidence that the Ipl1-Sli15 (Aurora kinase-INCENP) complex promotes chromosome bi-orientation by altering kinetochore-spindle pole connections. *Cell* **108**, 317-329.

Vader, G., Cruijsen, C. W., van Harn, T., Vromans, M. J., Medema, R. H. and Lens, S. M. (2007). The chromosomal passenger complex controls spindle checkpoint function independent from its role in correcting microtubule kinetochore interactions. *Mol. Biol. Cell* **18**, 4553-4564.

Westhorpe, F. G. A., Diez, M. A., Gurden, M. D., Tighe, A. and Taylor, S. S. (2010). Re-evaluating the role of Tao1 in the spindle checkpoint. *Chromosoma* **Feb 17.** [Epub ahead of print].

Wong, O. K. and Fang, G. (2007). Cdk1 phosphorylation of BubR1 controls spindle checkpoint arrest and Plk1-mediated formation of the 3F3/2 epitope. *J. Cell Biol.* **179**, 611-617.